Predicting processing parameters in High Temperature Laser Sintering (HT-LS) from powder properties

S. Berretta, K.E. Evans, O. Ghita

PII: S0264-1275(16)30589-5
DOI: doi: 10.1016/j.matdes.2016.04.097
Reference: JMADE 1749

To appear in:

Received date: 16 March 2016
Revised date: 27 April 2016
Accepted date: 28 April 2016

Please cite this article as: S. Berretta, K.E. Evans, O. Ghita, Predicting processing parameters in High Temperature Laser Sintering (HT-LS) from powder properties, (2016), doi: 10.1016/j.matdes.2016.04.097

Predicting processing parameters in High Temperature Laser Sintering (HT-LS) from powder properties

S. Berretta[1], K. E. Evans[1] and O. Ghita[1]

[1] *College of Engineering, Mathematics and Physical Science, University of Exeter, Exeter EX4 4QF, UK*

Abstract

New materials for Laser Sintering (LS) are usually developed using a trial and-error approach that consists of a series of builds within LS systems. This strategy is time consuming, costly and focuses only on the optimisation of the processing parameters, ignoring the powder properties of the materials under examination. Being able to predict processing parameters on the basis of the powder material properties would enable a faster development of new materials and new applications, while acknowledging a more in-depth understanding of the mechanisms involved in LS. This paper provides new results into the prediction of processing conditions from the material properties. It is here shown that high temperature polymers such as Poly Ether Ether Ketone (PEEK) and Poly Aryl Ether Ketone (PEK) can be successfully used in LS despite the lack of a super-cooling window. The evaluation of the stable sintering region of PEEK 450PF and the application the energy melt ratio parameter in relation to the mechanical performance of laser sintered PEEK samples are also provided. Lastly, a new method for estimating the powder bed temperature is proposed.

Keywords

PEK HP3, PEEK, Laser Sintering, Energy Melt Ratio, Stable Sintering Region, Super Cooling window

1 Introduction

Laser Sintering (LS) is a powder bed fusion additive manufacturing process where polymeric powders are consolidated layer upon layer by means of a CO_2 laser beam. In the process, polymer powders contained in the building chamber of a LS system are gradually heated up to a temperature (part bed temperature) where they can then be exposed to the laser. The latter will trigger the phase transition from solid to liquid phase using ideally the minimum input of laser energy. Once the laser exposure is finished, a new fresh layer of powder is spread and the laser exposure performed again. These operations are repeated until all desired components included in the build job are completed. At that point a long cooling phase will start.

When new materials are to be trialled in the LS process, the general approach for choosing the processing temperatures is based on qualitative criteria such as visual inspection of the powder bed for dark areas (hot spots) and cracks. If either occurs, approximate temperature adjustments such as changing the temperature by a few degrees within the LS system are applied. EOS [1], a top-leading manufacturer of LS equipment, provides a method for the evaluation of the optimum processing temperatures of PEK HP3 (EOS method). The steps of the EOS method for finding the optimum processing temperatures are the following: set the part bed processing temperature at 320 °C; deposit layers as per normal operation; pause build process, increase the part bed temperature by 5 °C, deposit one layer and wait for the heater power to drop below 40%; increase the part bed temperature by 5 °C to 330 °C, deposit one layer and wait for the heater power to drop below 50%; increase the part bed temperature in 2 °C increments, deposit one layer for each increment until the surface starts to discolour showing hotspots (melt of the material); reduce the temperature from this transition temperature, in 1-2 °C stages, deposit one layer for each increment until the hot spots stop to occur; set the exchangeable frame (temperature in the middle of the building chamber) and building platform (temperature at the bottom of a building chamber) temperatures at 20 and 25 °C below the part bed temperature.

Although reliable, this procedure could be greatly improved with a more accurate methodology.

The optimisation of the processing parameters for a desired part performance is instead based on an iteration of trial and error builds, where one parameter is changed at a time and its effect on the laser sintered part properties is evaluated through experimental mechanical and thermal testing.

Both strategies – the one for choosing the processing temperature and the other for optimising the processing parameters for enhanced part properties – can be highly time consuming and extremely expensive depending on the cost per kg of material being examined, its ability to be recycled, the physical size of the LS equipment available and the failure build risk of the system.

Polyamide (PA) based polymers are the most used polymers in the LS process. These plastics offer a wide super-cooling window [2], acceptable properties for a wide range of applications and are exhaustively used in prototyping. Their high recycle rate has allowed to margin the cost due to the trial-and-error builds and also promoted further development towards PA composites.

Recently a new generation of High Temperature (HT) polymers have entered the LS process. Examples are Poly Ether Ketone (PEK) and Poly Ether Ether Ketone (PEEK).These polymers provide superior mechanical, thermal and chemical performance than PA based polymers and therefore find application in high tech sectors such as defence, medical and oil and gas industries. Their unit cost is however significantly higher than PA based polymers and therefore it could be beneficial to formulate a method or a small set of experiments that are able to predict the processing temperature of an unknown material and identify the optimal set of processing parameters for a certain application *a priori,* i.e. before physical testing of powder within a HT-LS system.

A number of attempts to optimise the LS process are available in the literature. Ho et al. [3] evaluated the effect of the Energy Density (ED) parameter on polycarbonate structures, while a similar approach was adopted by Drummer et al. [4, 5] and Caulfield et al. [6] for the analysis of PA structures. Most of them focussed on the influence of ED on the mechanical performance of laser sintered parts and the main outcome from these studies was that an increase of the ED caused the mechanical properties, especially tensile strength, to improve up to a value where they stabilise or slightly decrease. Franco et al. [7, 8] modelled the LS process and quantified the correlation between ED and layer consolidation depth. Although some structures were laser sintered only for a feasibility purpose, rather than for mechanical characterisation, the authors offered a model of LS that includes processing parameters and fundamental material properties for the first time, unlike any of the previous models, which were based on the ED factor only.

More recently, Vasquez et al. [9] reported on the investigation of a parameter called Energy Melt Ratio (EMR), where material characteristics obtained by thermal analysis, gel permeation chromatography and thermo-gravimetrical analyses are used to predict the ideal LS processing parameters. “Ideal parameters” indicated those building settings that prevented material degradation during the laser consolidation while reaching the highest mechanical properties in the parts. Indeed, the authors built and mechanically tested samples at different EDs, calculated the corresponding values of EMR and then correlated these EMRs with mechanical and thermo-gravimetrical data. The EMR factor predicted well the parameters for which the material degradation started to occur during the LS process, especially for the PA 12 grade. Not surprisingly, the mechanical performance of the laser sintered samples under test improved with increasing values of ED and EMR, until it reached a peak value. Interestingly, the EMR value predicting material degradation was found to be relatively close to the highest limit value of the tensile strength. These findings also allowed the authors to identify a new temperature region for LS based on material properties called “Stable sintering region”. This temperature interval is based on the melt and degradation behaviour of the powders and should guide the choice of the processing temperature and laser parameters during a LS building operation. The EMR combined with the evaluation of the stable sintering region can help to reduce significantly the number of preliminary builds for a new material development and optimisation. However, a small number of build trials for a specific material will still have to be carried out.

The aim of this paper is to predict for HT polymers the processing temperature such as the part bed temperature and the laser exposure parameters from the powder properties. At present, a study into the development and optimisation for predicting processing parameters of the PEEK material within the only HT-LS commercial system EOSINT P 800 is still missing and therefore it constitutes the main investigation of this work. HT-LS can provide PEEK components for high demanding

engineering applications in a wide range of industrial areas such as aerospace, automotive and medical industries. HT-LS of PEEK also relies on a lower processing temperature window than PEK, the current commercial HT-LS material, due to a 30˚ C lower melting temperature between PEK and PEEK. Experimental studies on laser sintering of PEEK are not the main topic of this paper and can be found elsewhere [10-12].

2 Theory

2.1 Super-cooling window

The super-cooling window is the LS processing window defined based on the Differential Scanning Calorimetry (DSC) thermoscan of the powder under test [13], largely used in the LS community [14-17]. This window is defined as the temperature gap between the onset of the melting event and the onset of the crystallisation event. This window essentially constitutes a wide range of temperature values that can be used as a processing temperature inside a LS system for successful LS manufacturing. This spectrum should ensure that the powder lying in the powder bed of a generic LS system does not melt before exposure to the laser and does not crystallise during laser exposure.

2.2 Stable Sintering region

The stable sintering region is a concept introduced by Vasquez et al. [9] to study established and new potential LS materials in the region above their melting points and below their degradation temperatures. It aims to predict the temperature interval that leads to thermal degradation of the material in order to avoid it, during a LS building operation, especially during the laser exposure. The stable sintering region is bounded by values found with DSC, hot stage microscopy and Thermo-Gravimetrical Analysis (TGA) of polymeric powders. The lower limit is the temperature at which the material is fully molten and is found with the combination of DSC data (melting peak temperature) and hot stage testing (temperature at which the powder particles were fully melted). The upper limit is the temperature at which the 1% weight loss degradation occurs during a TGA experiment that is carried out from room temperature to HT at a heating rate of 10 ˚C x min^{-1}. This method clearly does not take into account the crystallisation effect present in semi-crystalline polymers such as PA based powders or PAEK materials and therefore according to Vasquez et al. [9] can be used for more types of polymers. The authors showed that PA 12 presents a stable sintering region at 120˚C, with lower limit at 200˚C and upper limit at 320˚C. The processing parameters of the laser exposure during LS - laser power, scan spacing, scan count and laser speed - should therefore increase the temperature of the powder particles in the powder bed above 200˚C in order to achieve complete melting, but remain below 320˚C in order to avoid their thermal degradation [18].

2.3 Energy Melt Ratio

During a LS building operation, a laser exposes defined areas in the powder bed, triggering the melting of the material particles interested. In this operation, the laser is believed to fully transfer an amount of energy into the powder bed that depends on the characteristics of the laser exposure. Moreover, in order to achieve a specific successful sintering in only the laser exposed areas of the powder bed (and not across all the powder bed) the powder bed is kept at a temperature that is just below the material melting temperature.

The characteristics of the laser exposure are generally grouped under the "Energy Density" (ED) parameter which is defined (Eq.1) by the laser power (P), the number of times the same region is exposed by the laser ("Scan count", C), the distance between two next segments of laser exposure ("Scan spacing", S) and the laser beam velocity or laser speed (v). ED is therefore directly proportional to the laser power and inversely related to its velocity and scan spacing.

$$ED = \frac{P\,C}{S\,v} \qquad [\frac{J}{mm^2}] \qquad \text{Eq.1}$$

When the laser energy takes into account the powder layer thickness (z)set in a given build, the laser energy becomes a volume energy density (ED_{vol}), as shown in Eq.2.

$$ED_{vol} = \frac{ED}{z} \qquad [\frac{J}{mm^3}] \qquad \text{Eq.2}$$

From the point of view of the material, the volume energy required to melt the powder material (E_m) in the building chamber depends on its specific heat capacity (C_p), melting temperature (T_m), LS powder bed temperature (T_b), enthalpy of melting (h_f), bulk density (Q) and packing fraction (Φ) (Eq. 3).

$$E_m = \left[C_p\,(T_m - T_b) + h_f\right] Q\,\Phi \qquad [\frac{J}{mm^3}] \qquad \text{Eq.3}$$

The Energy Melt Ratio (EMR) is a numerical parameter introduced by Starr et al. [19] and later investigated by Vasquez et al. [9], used to study the relationship between LS manufacturing parameters and mechanical properties of laser sintered PA specimens. The parameter describes the ratio between the energy applied in LS (ED_{vol}) and the energy required to melt a unit volume of a given material (E_m) (Eq.4).

$$EMR = \frac{ED_{vol}}{E_m} = \frac{ED}{E_m\,z} = \frac{\frac{P\,C}{S\,v}}{\left[C_p\,(T_m - T_b) + h_f\right] Q\,\Phi\,z} \qquad [1] \qquad \text{Eq. 4}$$

At present, EMR is the most comprehensive factor that couples processing parameters with powder properties. EMR does not have absolute minimum and maximum limits; a high value of EMR means that the amount of energy applied through the LS processing setting is far higher than the energy required theoretically to melt that specific material, but it does not necessary imply that the processing parameters are inducing degradation in the powder material. Starr et al. [19] utilised the EMR in parallel with the mechanical properties of laser sintered PA samples manufactured at increasing values of ED_{vol}. Mechanical properties such as yield stress increased with increasing values of ED_{vol} and EMR until it stabilised at EMR value of approximately 2.

However, EMR can also be formulated and solved for those processing parameters that lead to material degradation so that degradation during laser exposure can be avoided. With this intent, Vasquez et al. [9] defined the EMR for material degradation (EMR_D) (Eq.5) in the LS process using the volumetric energy density for degradation ($ED_{vol,D}$), the volume energy required to melt the powder material (E_m) and theoretical energy of degradation (per unit volume) (E_D).

$$EMR_D = \frac{ED_{vol,D}}{E_m} = \frac{E_D}{E_m} \qquad \text{Eq.5}$$

The theoretical volume energy necessary to induce degradation of a given material (E_D) is defined by specific heat capacity (C_p), onset degradation temperature (T_D), melting temperature (T_m) activation energy for degradation (E_A), molecular weight (M_W) and material density (Q) (Eq.6).

$$E_D = [C_p(T_D - T_m) + \frac{E_A}{M_w}]\, Q \qquad [\frac{J}{mm^3}] \qquad \text{Eq.6}$$

The processing parameters leading to degradation during a LS build process are found by combining Eq.4, 5 and 6. Following the energy density equation 1 but for degradation, the laser power for degradation is defined by Eq. 7.

$$P_D = \frac{EMR_D\, E_m\, S\, \nu\, z}{C} \qquad [W] \qquad \text{Eq.7}$$

In this work, the parameters used in the evaluation of the EMR values have been, when possible, evaluated experimentally or found in the literature otherwise. The measurement of the activation energy (E_A) has been quantified through the Kissinger method. This method and its assumptions can be found elsewhere [20] and therefore are not reported here. The aim of this paper is to show whether EMR can be used to predict the processing temperature and laser exposure parameters for HT polymers in LS based on their powder properties.

3 Experimental work

The aims of this work are to attempt to predict part bed temperature and optimal laser exposure parameters from powder properties.

The prediction of the part bed temperature is carried out only on powder samples and is based on thermal analysis of the material properties and the temperature settings currently used in LS systems.

The powders and laser sintered samples are used for prediction of the laser exposure parameters that will not lead to the polymer degradation during processing, while allowing to achieve high mechanical performance by combining diverse techniques: DSC, Tensile testing and TGA.

3.1 Materials

The materials used for the prediction of the part bed temperature are Poly Ether Ether Ketone (PEEK) and Poly Ether Ketone (PEK) from the Poly Aryl Ether Ketone (PAEK) family, polyamide (PA) 12 and 11 from the PA family. PEK and PEEK exhibit high mechanical performance, elevated thermal and chemical resistance and important mechanical performance [21]. They are inherently flame retardant and have excellent wear resistance. PEK HP3, supplied by EOS [22], has a melting temperature of 373˚C [22]. Two types of the PEEK polymer, PEEK 150PF and 450PF, both supplied by Victrex [23], have been used. Both materials present a melting temperature of 343 ˚C. In comparison with PEK, PEEK presents a lower melting temperature and a lower glass transition temperature - therefore potentially a better processability - with the same 250 ˚C operating temperature of PEK. The principal difference between the two grades of PEEK used in this work is the material viscosity [24]. In order to improve their flowability, the PEEK 150PF and 450PF powders were thermally conditioned according to Leuterer et al. [25] before use in the HT-LS. Details on this procedure and its effect on the material properties can be found elsewhere [10, 26]. PA 2200 is a PA 12 based powder while PA 1101 is a PA 11 based powder, both are supplied by EOS [22]. PA 2200 has a

melting temperature 176 ˚C [27]. Available in a discrete number of composite materials optimised for LS, PA 2200 is one of the most well established materials for LS. One of the main advantages of this material is its high recyclability to a content up to 50% by weight for a new generic LS process [28]. PA 1101 instead exhibits a melting temperature of 201 ˚C [27].

The prediction of optimal building parameters includes the evaluation of the Stable Sintering region and the calculation of the EMR values using PEEK 450PF.

3.2 Differential Scanning Calorimetry (DSC)

DSC allows the study of a wide range of thermal properties of materials. Onset melting and onset crystallisation temperatures of powder samples were analysed using the Mettler Toledo DSC 821e/700 with sample weight of approximately 10 mg. The powders were heated from room temperature above their melting temperature (200 ˚C for PA polymers and 400 ˚C for PAEK powders) with heating and cooling rates of 10 ˚C x min^{-1}. Nitrogen was used as protective gas at a flow rate of 50 ml x min^{-1}. The evaluation of the thermal properties has been assessed by using the STARe package software. Onset melting and crystallisation temperatures, defined as "the intersection point of the signal baseline after transition and the inflectional tangent", were calculated according the corresponding onset tool available in the STARe software [29]. The first derivative has been evaluated automatically on the heating segment of an entire DSC thermoscan using the "first derivative" tool in the STARe software. A minimum number of three measurements were carried out for every material analysed.

The DSC scan used in the evaluation of the stable sintering region was carried out on thermally conditioned PEEK 450PF powder sample of mass approximately equal to 10 mg. The sample was heated from room temperature to 400 ˚C at 10 ˚C x min^{-1} with purge gas flow (nitrogen) of 50 ml x min^{-1}. Melting temperature and enthalpy of melt of PEEK 450PF used in the EMR were also found with this method.

3.3 HT-LS manufacture

HT laser sintered components of PEEK 450PF were produced under different laser exposure settings. The specimens were manufactured with increasing values of ED and tested in terms of tensile strength as reported by the authors in a previous work [10]. For clarity, ED data and tensile strength results are reported in Table 1.

Processing parameters profile name	**Processing parameters**		**Tensile Strength [MPa]**
	v = 2550 mm s^{-1} S = 0.2 mm	**ED [J mm^{-2}]**	
	P (W)		
Build 1	7.5	0.015	31 ± 4
Build 2	9.0	0.018	44 ± 4
Build 3	12.0	0.024	59 ± 6
Build 4	13.5	0.026	64 ± 5

Build 5	15.0	0.029	63 ± 5
Build 6	16.5	0.032	67 ± 4

Table 1. Processing parameters and ED used for PEEK 450PF manufacture [10]

3.4 Thermo-Gravimetric Analysis (TGA)

TGA is an analytical technique used for the study of thermal degradation phenomena on materials. The TGA data used for the evaluation of the stable sintering region and the calculation of the onset temperature degradation used in EMR_D were performed on PEEK 450PF powder samples (sample mass of approximately 10 mg) heated from room temperature to 900 ˚C at a heating rate of 10 ˚C x min^{-1} using the Mettler Toledo TGA/DSC 1-1100 ˚C. Nitrogen was used as protective gas at 50 ml x min^{-1} flow rate. The same method was used for the evaluation of the onset degradation temperature HT laser sintered PEEK 450PF sample manufactured with the processing parameters from build 3 (Table 1) and thermally conditioned PEEK 450PF powder. All the data analysis was performed by using the STARe package software.

3.5 Kissinger method and evaluation of the activation energy

The Kissinger method allows to measure the activation energy (E_A) leading to material thermal degradation by performing several TGA experiments carried out at different heating rates (β), - every experiment at a different heating rate - . The exothermic peak temperature (T_{max}) was recorded at varying heating rates and the data were used for the evaluation for a straight line fit in the plot having the factor $\ln\frac{\beta}{T_{max}^2}$ as Y axis and the parameter $\frac{1000}{T_{max}}$ as X axis. The slope of the straight line multiplied by the gas constant (R = 8.314 J x mol^{-1} x K^{-1}) is the activation energy value for thermal degradation of the material analysed. T_{max} has been measured by evaluating the peak of the first derivative of the TGA results within the STARe software. The heating rates of 5, 10, 15 and 20 K x min^{-1} were used for the evaluation of the activation energy E_A of PEEK 450PF.

3.6 Packing fraction measurement

The bulk density is the density of loose and uncompressed powder per unit volume. The packing fraction is a numerical parameter that indicates how well a bulk material (powder or grain) can compact, i.e. occupying the smallest volume with the highest number of particles. When this value is close to zero indicates that a material has poor packing behaviour with many voids within the unit volume. When instead it is close to 1 the material has good packing performance with a large number of particles occupying the unit volume and very few or nil voids. This parameter represents a key property in powder bed fusion processes because a good degree of compaction in the powder bed is necessary for the creation of fully dense components. The measurement of the bulk density consisted of weighing a known volume (100 cm^3) of material. The value of the packing fraction of thermally conditioned PEEK 450PF has been measured by evaluation of the ratio between the bulk density of the powder and the true density of the material of 1320 kg x m^{-3} [30, 31]. The details of this method are reported elsewhere [32].

3.7 Energy melt ratio

The values utilised for the degradation limit EMR_D (Eq. 5) in paragraph 4.5.3 are shown in Table 2.

Parameter name	Parameter	Value
Specific heat capacity	C_p	2200 kJ Kg^{-1} $^{\circ}C^{-1}$[31]
Onset degradation temperature (1% weight loss)	T_D	559.97 ˚C
Melting peak temperature	T_m	339 ˚C
Energy of activation	E_A	249. 7 kJ mol^{-1}
Molecular weight	M_W	155000 g mol^{-1} [33]
Bulk density	Q	0.383 [25]
Scan count	C	1
Scan spacing	S	0.2 mm [1]
Laser speed	v	2550 mm s^{-1} [1]
Layer thickness	z	0.12 mm

Table 2. Material and HT-LS processing parameters utilised for the evaluation of the EMR value leading to degradation for the thermally conditioned PEEK 450PF powder

The values used for the evaluation of the EMR corresponding to different processing parameters (Eq 4) of laser sintered PEEK 450PF samples presented in paragraph 4.5.4 are reported in Table 3.

Parameter name	Parameter	Value
Specific heat capacity	C_p	2200 kJ Kg^{-1} $^{\circ}C^{-1}$ [31]
Part bed temperature	T_b	332 ˚C
Melting peak temperature	T_m	339 ˚C
Enthalpy of melting	h_f	58.6 J g^{-1}
Bulk density	Q	0.383 g cm^{-3}
Packing fraction	Φ	0.29
Scan count	C	1
Scan spacing	S	0.2 mm [1]
Laser speed	v	2550 mm s^{-1} [1]
Layer thickness	z	0.12 mm
Laser powers used for sample manufacture (Table 1)	$P_1 – P_6$	7.5, 9, 12, 13.5, 15.0,16.5 W

Table 3. Values used for EMR related to varied manufacturing parameters

4 Results

4.1 Thermal properties of established LS powders and powder bed temperatures

The melting and crystallisation onset temperatures have been evaluated for established LS material such as PA 2200, 50/50 PA 2200, PA 1101 and PEK HP3, and for thermally conditioned PEEK 450PF and 150PF. The purpose of these analyses was to provide the information required for predicting processing temperature methods. PA based materials and PEK HP3 were used as benchmark materials. The onset melting and crystallisation temperatures of the powders are listed in Table 4. The part bed temperature (T_b) represents the temperature at which the powder is held before the laser exposure. The thermal values of the established LS materials are listed in Table 4 along with the part bed temperatures found by applying the traditional method of eye inspection EOS method [1].

Material	LS/HT-LS system	T_b (˚C)	Onset Melting Temperature (˚C)	Onset Crystallisation Temperature (˚C)
PA 2200 virgin	EOSINT P 100	168-169	180.6 ± 0.7	151.8 ± 0.3
PA 2200 50/50 virgin/used	EOSINT P 100	168-169	179.4 ± 0.2	150.6 ± 0.5
PA 1101	EOSINT P 100	185	197.6 ± 1.0	165.8 ± 0.3
PEK HP3	EOSINT P 800	365	354.2 ± 5.3	338.3 ± 0.4
PEEK 150PF	EOSINT P 800	338	333.7 ± 5.2	313.4 ± 0.2
PEEK 450PF	EOSINT P 800	332	320.5 ± 0.4	300.2 ± 0.5

Table 4. Part bed temperatures and thermal properties of optimised LS materials and thermally conditioned PEEK grades

It must to be specified that only the thermally treated PEEK 150PF and 450PF powders are included in the analysis as the two powder grades were not spreading well during the HT-LS process in the 'as received' condition. As expected, the PA grades show lower melting and crystallisation onset temperature than the HT polymers (PEK HP3 and PEEK grades). Interestingly, no significant temperature shift and enthalpy change seem to occur between PA 2200 and 50/50% virgin/used PA 2200 grades. By comparing the thermal properties of the powders with their corresponding part bed temperatures (Table 4) it is possible to notice that the part bed temperatures of the PA based grades are below their onset melting temperatures. On the contrary, the part bed temperature of PEK HP3 and thermally conditioned PEEK materials is higher than the onset temperature of melting. This is an interesting result as it proves that the HT-LS materials are processed in the EOSINT P 800 system at a temperature where material melting should have already started according to DSC analysis.

4.2 Super-cooling window

The super-cooling window has been evaluated experimentally using DSC analysis on established LS materials such as virgin PA 2200, 50 /50 used/ virgin PA 2200, PA 1101 and PEK HP3, and on thermally conditioned PEEK 150PF and 450PF grades. Figure 1 shows the DSC thermoscans of virgin PA 2200, 50/50 virgin /used PA 2200 and PA1101.

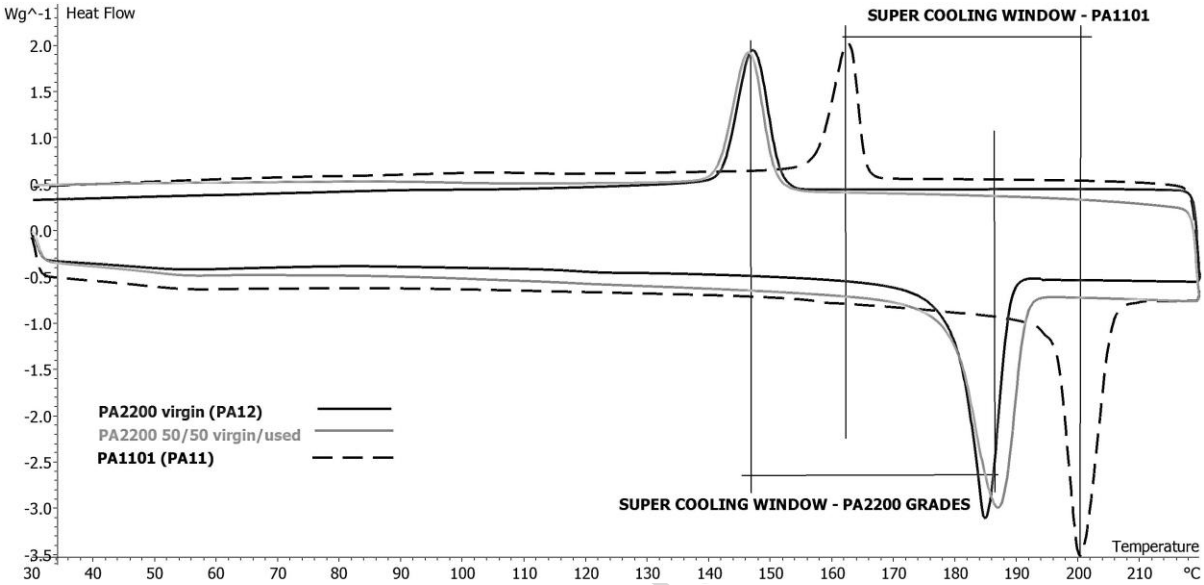

Figure 1. DSC thermoscan showing the super-cooling window applied to PA 2200 powders, virgin and 50/50 virgin/used, and to PA 1101

Both mixtures of PA 2200 and PA 1101 (Figure 1) exhibit the super-cooling window. A wide temperature range is clearly visible between the onset of the melting phenomenon and the onset of the crystallisation event for these three grades. Both PA 2200 and PA 1101 grades also show sharp, well defined melting and crystallisation peaks. These characteristics are well-known in the LS community and they have been considered to be the reason why PA-based materials can be successfully laser sintered. The super-cooling window method can be fully validated for these three materials by noticing that the LS part bed temperature of these materials, shown in Table 4, are located within the onset melting and the onset crystallisation temperatures, the temperature interval defined by the super-cooling window.

Figure 2 shows the DSC thermoscans of PEK HP3, thermally conditioned PEEK 450PF and 150PF.

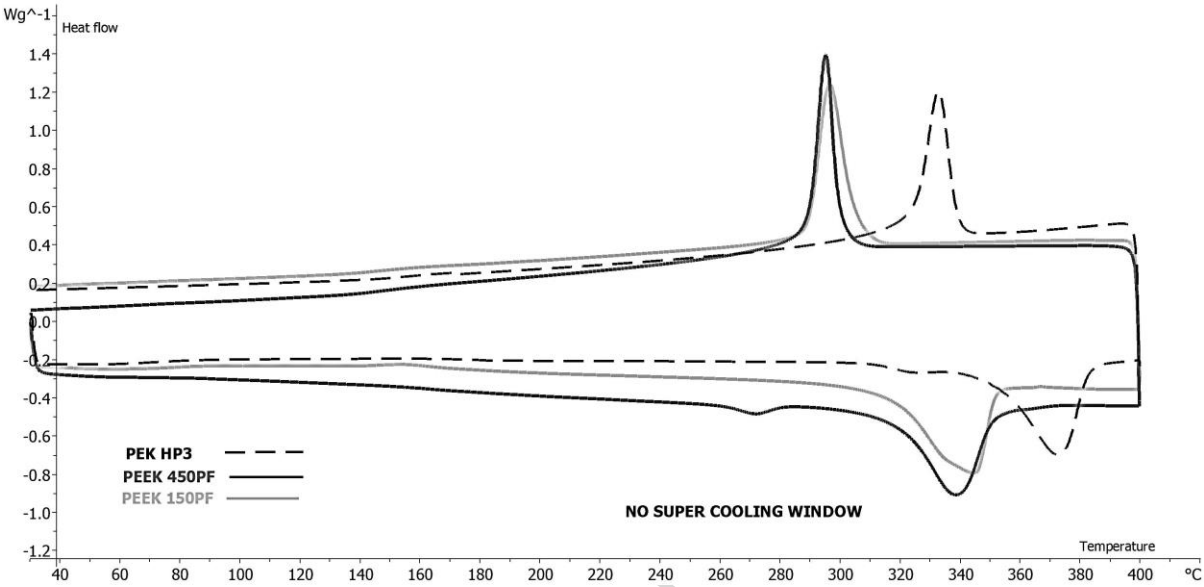

Figure 2. DSC thermoscan showing that the super-cooling window does not apply to PEK HP3

The melting and crystallisation areas of PEK HP3 are broad and overlap indicating the lack of temperature gap between the onset of the melting region and the onset of the crystallisation phase (Figure 2). The super-cooling window does not seem to exist for this material. Similar to PEK HP3, thermally conditioned PEEK powders (150PF and 450PF) do not exhibit the super-cooling window; the melting and crystallisation regions widely overlap. These results are not surprising, as it was noted earlier (4.1.1) that the part bed processing temperatures of these materials within the HT-LS system EOSINT P 800 were inside the melting region.

Clearly, the super-cooling window can help to approximately estimate LS processing temperatures of PA based material such as PA 2200, 50/50 PA 2200 and PA1101. However, it cannot be considered the only method to select new LS material candidates as polymers that do not exhibit a clear temperature interval between melting and crystallisation regions can be still laser sintered. This is the case of amorphous, elastomers and HT polymers such as PEK HP3, which are currently commercially applied in LS.

4.3 The first derivative method

A new, simple approach to estimate the part bed temperature for HT-LS PAEK materials is proposed here. This method consists of evaluating the 1st derivative of the heating segment of a DSC thermoscan of the PAEK material under test and calculating the minimum point. The aim of this technique is to replace a process involving qualitative judgement during a LS build with a more "automatic" quantitative and predictive technique.

The 1st derivative data of PA 2200 grades (virgin and 50/50% used/virgin) and PA1101 are shown in Figure 3 and 4. The processing temperature (part bed temperature) of these materials is lower than the minimum temperature found with the first derivative method. This result is not surprising as the processing temperature of PA 12 and 11 is lower than the onset of the melting region (Table 4). The first derivative method is therefore not useful for this group of polymers.

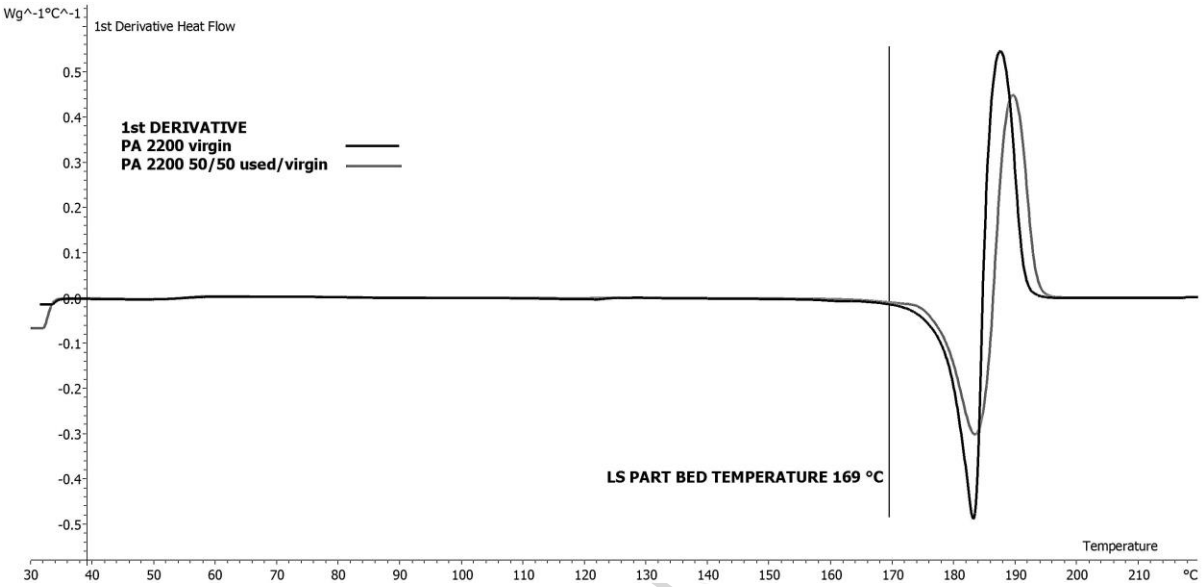

Figure 3. 1st Derivative of the melting segment of the DSC thermoscan of PA 2200 grades

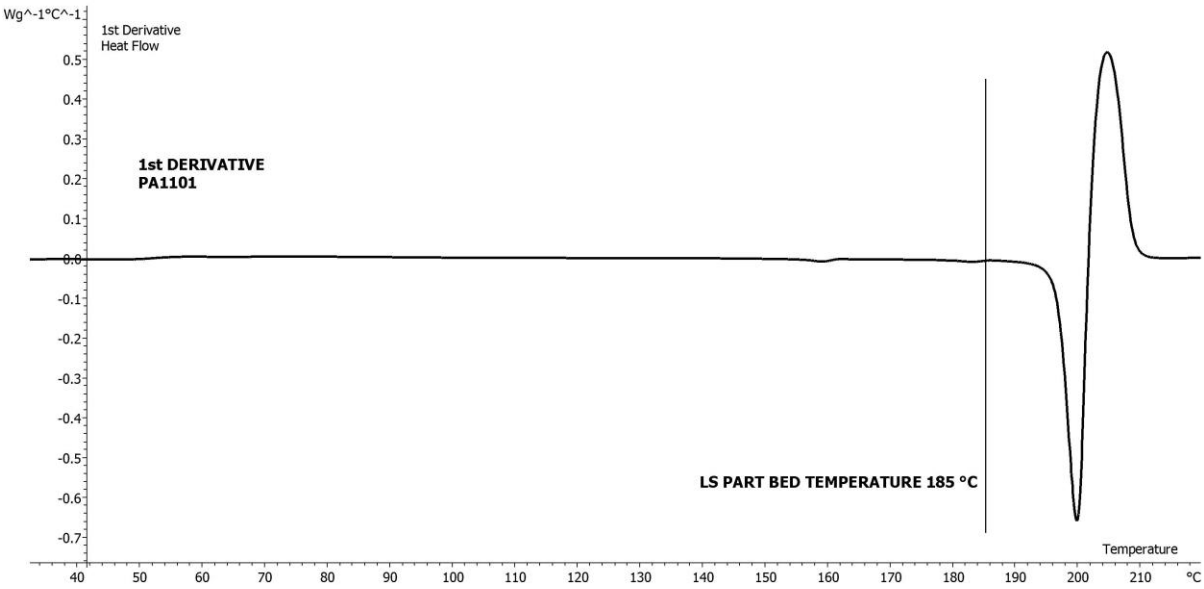

Figure 4. 1st Derivative of the melting segment of the DSC thermoscan of PA 1101 grade

The first derivative of PEK HP3, thermally conditioned PEEK 150PF and 450PF are shown from Figure 5 to Figure 7.

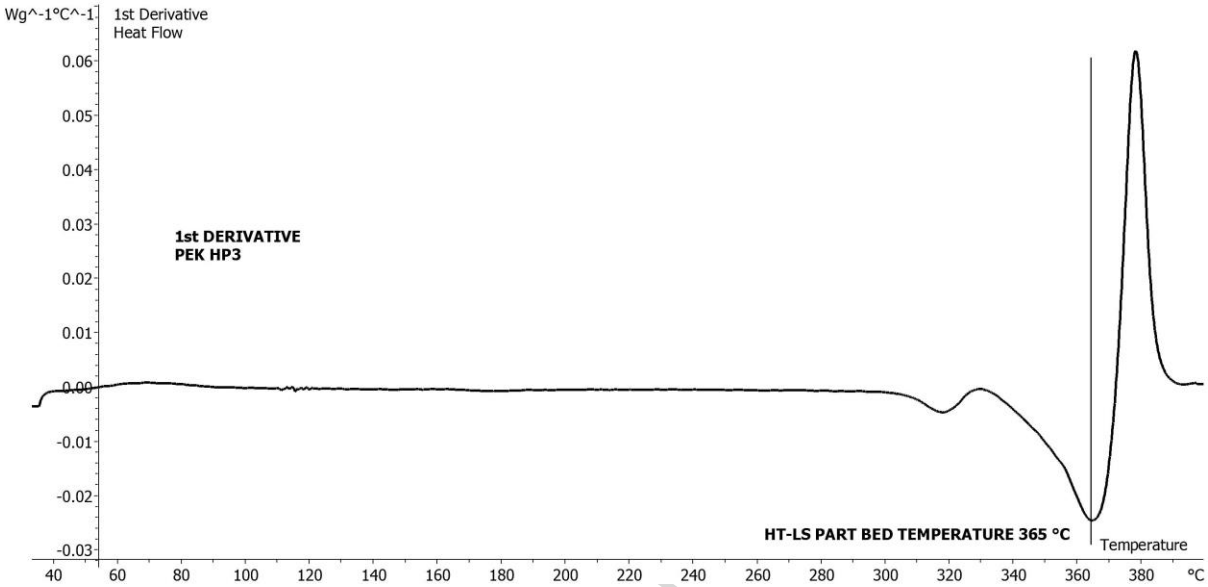

Figure 5. 1st Derivative of the melting segment of the DSC thermoscan of PEK HP3

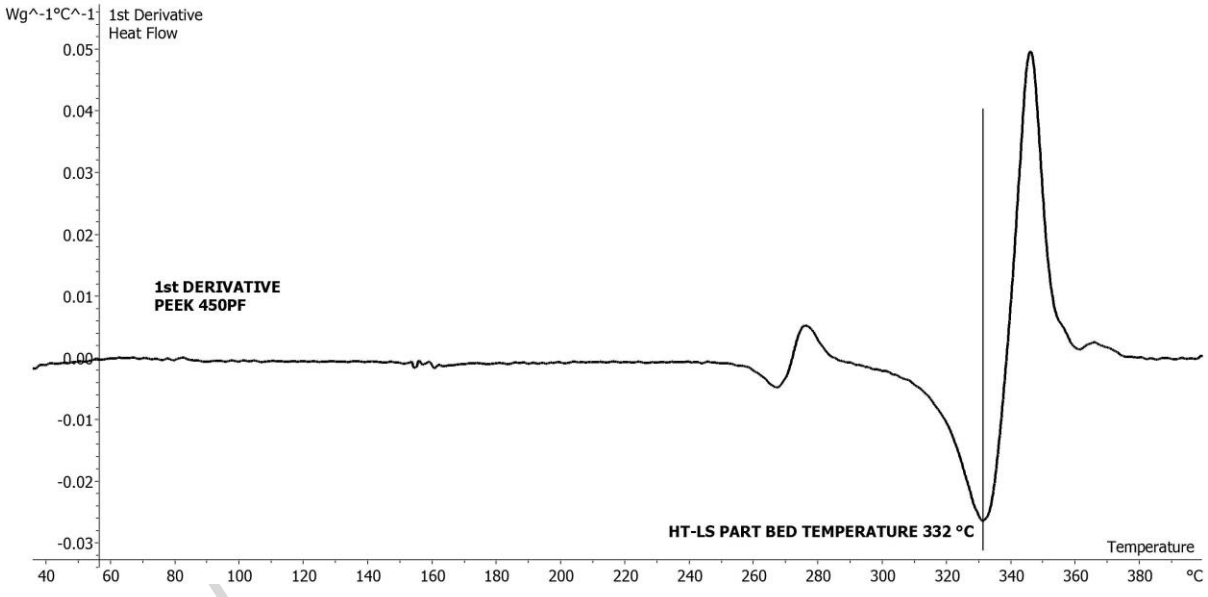

Figure 6. 1st Derivative of the melting segment of the DSC thermoscan of the thermally conditioned PEEK 450PF

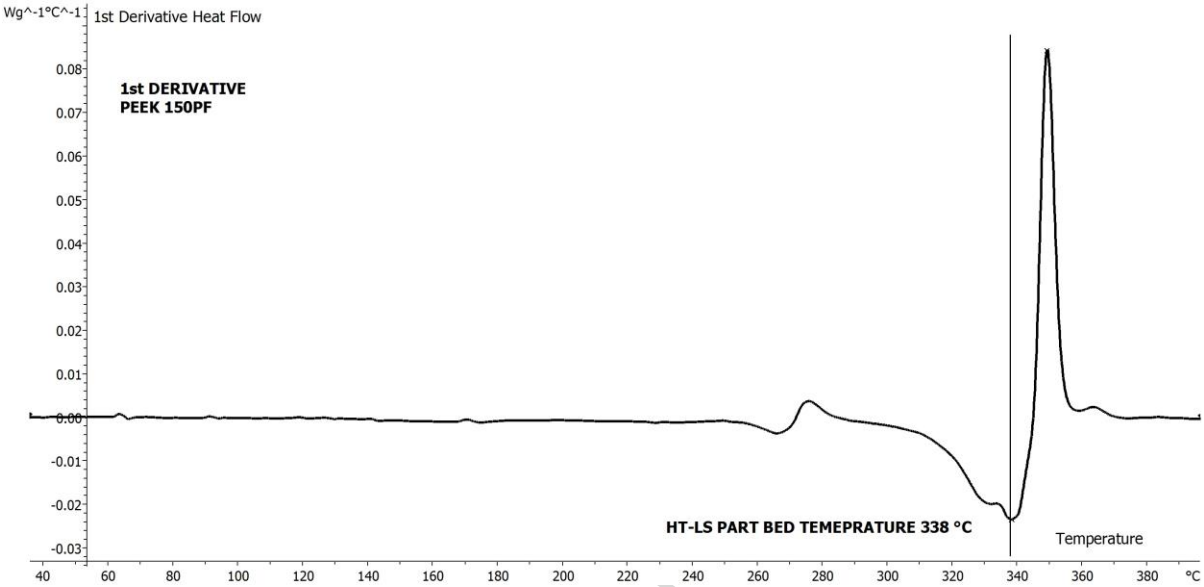

Figure 7. 1st Derivative of the melting segment of the DSC thermoscan of the thermally conditioned PEEK 150PF

The minimum of the first derivative curve of the DSC thermoscans of the HT polymers (Figure 5 to Figure 7) is equivalent to the corresponding HT-LS part bed processing temperature. The mean values of the minimum and maximum values of the 1st derivative obtained by the multiple tests carried out on all the three materials are listed in Table 5 in parallel with the corresponding part bed temperatures determined through the standard trial and error approach within the HT-LS system EOSINT P 800.

Material	Min (˚C)	Max (˚C)	Part bed temperature
PEK HP3	366 ± 2	379 ± 1	365 ˚C
PEEK 150PF	341 ± 3	350 ± 1	338 ˚C
PEEK 450PF	332 ± 1	346 ± 1	332 ˚C

Table 5. Thermal properties of the 1st derivative of the melting segment of the DSC thermoscans (average values and standard deviations)

It is shown that the part bed temperature required for successful HT-LS within the EOSINT P 800 system seems to equate to the minimum of the first derivative. The part bed temperature used for processing PEEK 150PF is slightly outside the average minimum value found in the 1st derivative, nut still included in the corresponding interval error. The materials show standard deviations of 1to 3°C that could depend on the two different types of thermal tests (DSC and LS processing), different material volumes, and different methods of controlling and monitoring temperatures.

The reason why the part bed temperature equates to a minimum point in the first derivative can be explained by understanding the meaning of the first derivative of the heat flow signal of a DSC thermoscan. A DSC thermoscan shows how the heat flow for a given material changes over a thermal profile. The 1st derivative represents the heat flow rate, i.e. how the heat changes due to absorption or release by the material are over a given thermal profile. In our heating segments, the

minimum point of the 1st derivative represents the point at which a further temperature increase will provoke the highest gradient in the heat flow as a sign of melting (melting peak). The use of the 1st derivative therefore helps to find the point (temperature) where the minimum energy introduced by the laser into the material will trigger its melting. The use of derivatives in DSC data analysis for better data analysis has been reported also by Bouzidi et al. [34]. The authors showed that the use of first and second derivatives of DSC thermoscans can help to discriminate overlapping events in the transition regions (glass transition region, crystallisation and melting) that would not be visible in the original data. Gabbott [35] instead recommends to use the second derivatives especially for identifying the correct onset and endset of thermal transition events. For clarity, the combined analysis of original data, 1st derivative and 2nd derivative of PA1101 and PEEK 150PF are shown in Figure 8 and Figure 9.

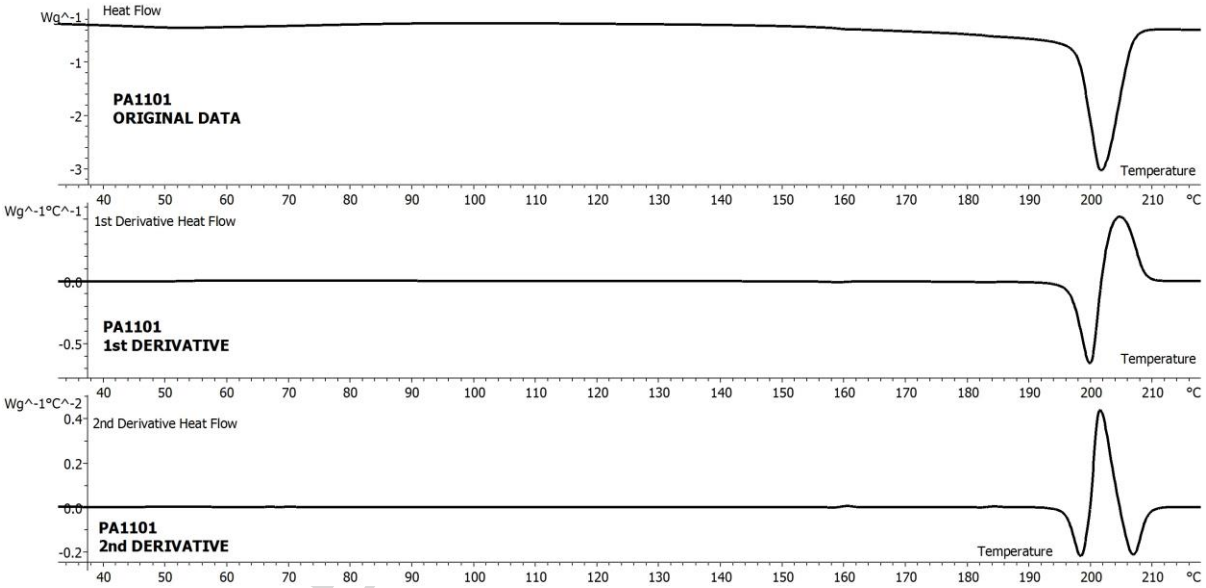

Figure 8. DSC thermoscan of PA1101 combined with first and second derivatives

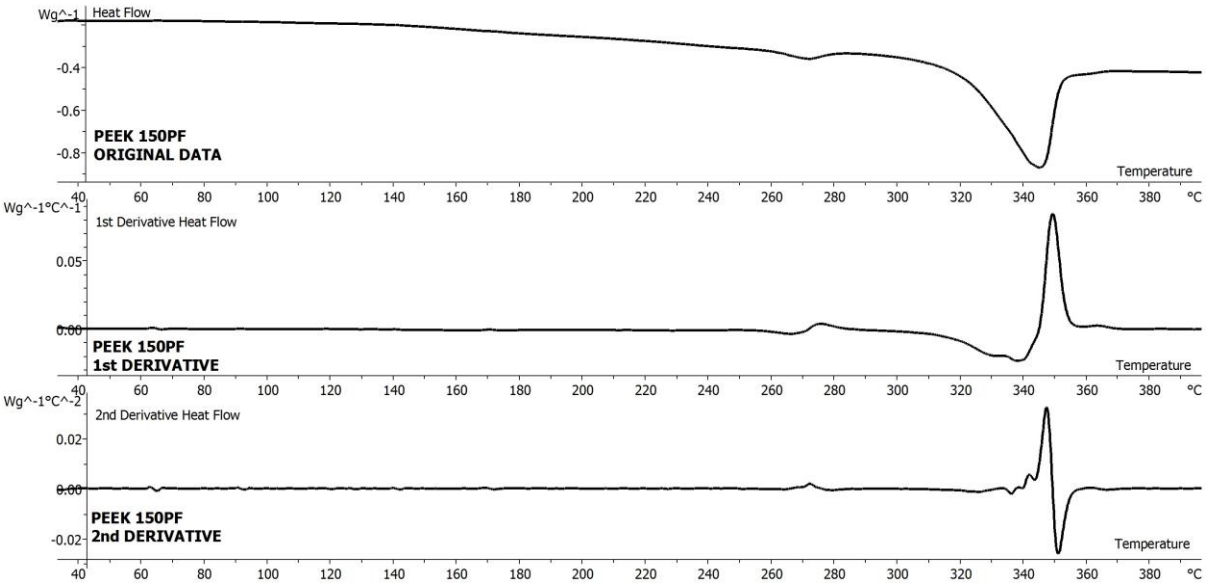

Figure 9. DSC thermoscan of PEEK 150PF combined with 1st and 2nd derivatives

In Figure 8, the second derivative of the thermoscan of PA1101 helps to better identify the onset and endset of the melting region and both derivatives confirm the presence of one melting peak in the melting region. In the case of PEEK 150PF instead (Figure 9) the first and second derivatives clearly show the presence of overlapping events in the melting region. These results emphasise how complex the thermal behaviour of PEEK is and can also be the reason for the observed correlation between the minimum value of the 1st derivative and the bed temperature. Fundamental studies carried out on the crystal structure of PEEK showed the possibility of having two populations of lamellar thickness [36-38]. Recently, Wang et al. [39] identified also two types of nano-sized crystal blocks self-organized into a spherulitic structure in PEEK. However, other studies believe that the double melting behavior of PEEK is related with the melting–recrystallization effect. In order to further validate the results from the first derivative technique, samples of PA1101, PEEK 150PF and PEEK 450PF have been subjected to different thermal profile within DSC analysis. More precisely samples of PA1101 have been heated at a heating rate of 10 °C/min from room temperature to 185°C (part bed temperature in a LS machine), 190°C temperature at which according to heat flow and first derivative (Figure 8) melting has not started yet and at 200 °C (approximately the melting peak).PEEK 150PF powders have been heated at a heating rate of 10 °C/min from room temperature to 338 °C (part bed temperature and approximate minimum of the first derivative) and to 345 °C (temperature outside the interval error suggested by the first derivative technique). PEEK 450PF samples have been heated from room temperature to 332°C (part bed temperature and minimum in the first derivative) and at 340°C (temperature well outside the interval error suggested by the first derivative technique) at a heating rate of 10 °C/min. All the samples have then been inspected and the pictures are shown from Figure 10 to Figure 12.

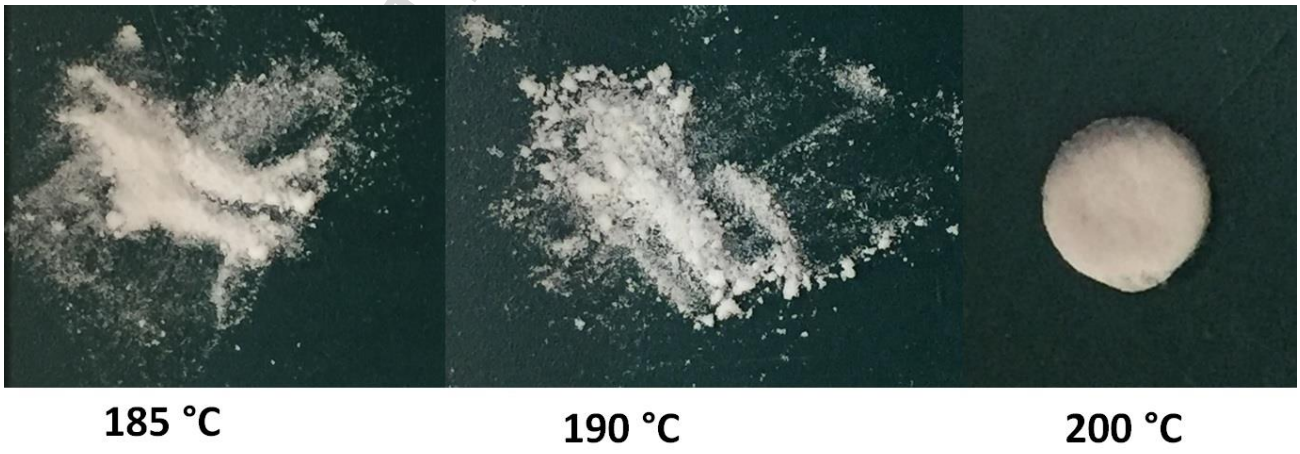

Figure 10. PA1101 powder heated from room temperature to 185, 190 and 200 °C using DSC

Figure 11. PEEK 150PF samples heated from room temperature to 338 and 345 °C using DSC

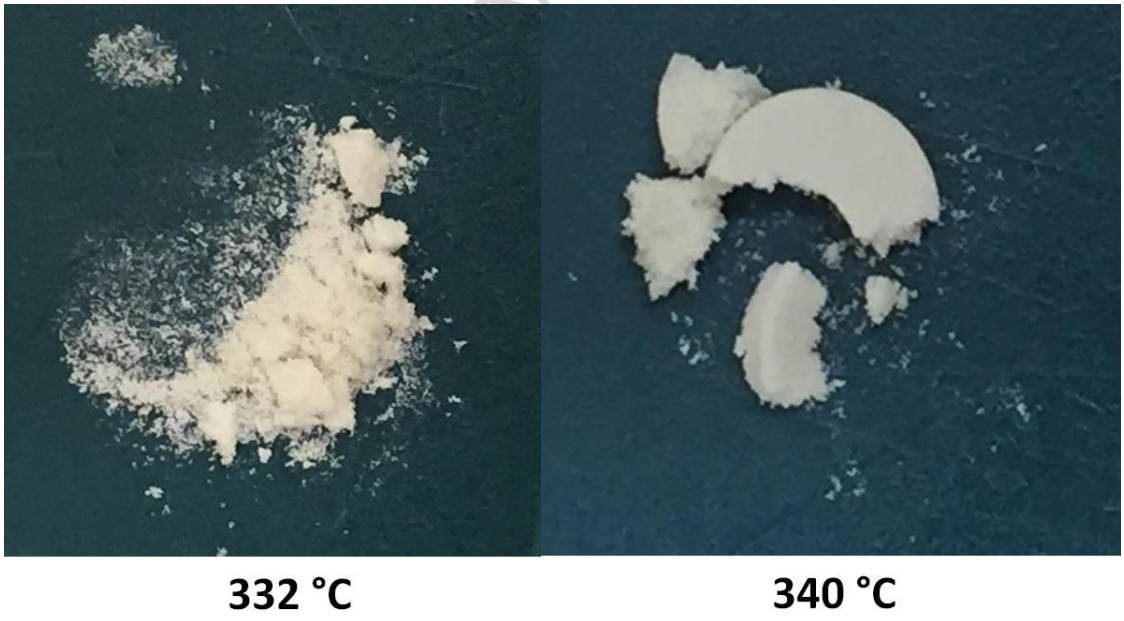

Figure 12. PEEK 450PF samples heated from room temperature to 332 and 340 °C using DSC

Figure 10 shows how PA1101 powder does not start to melt until the 200 °C temperature is reached, PEEK 150PF appears to start consolidating above the interval error of the minimum found with its first derivative, thus confirming the validity of this method (Figure 11). Similarly to PEEK 150PF, PEEK 450PF is still in powder form at the temperature found with the first derivative technique and seems to start melting at 340°C (Figure 12).Although basic, it seems therefore that the use of the first derivative for polymers with broad melting regions such as poly aryl ether ketones polymers provides a good estimate of the part bed temperature for PEK HP3, PEEK 150PF and 450PF from the powder properties and offers the opportunity to reduce the number of builds involved in the development of a new LS material. It is also interesting to notice that the temperatures suggested with this technique are not relevant to only the commercial HT-LS system EOSINT P800 but also

correspond to the part bed temperature found by previous researchers when laser sintering PEEK in modified standard LS systems [11, 40]. Schmidt et al. [11] for example laser sintered PEEK in a PA 12 machine incorporated with an in-lab designed heating dome that according to the authors should have allowed to reach higher temperatures in the building chamber than those used for LS PA12. Thin samples were manufactured and tested in terms of hardness.

In an ideal scenario more high temperature polymers should be tested with the first derivative technique, but the number of high temperature polymer powder grades suitable for LS is limited commercially, even at development stage.

4.4 Stable sintering region

The evaluation of the stable sintering region for thermally conditioned PEEK 450PF is shown in Figure 13. The black line represents the TGA data "Weight loss", while the dash trace is the heat flow signal resulting from DSC analysis ("Heat flow"). As hot stage testing was not carried out for PEEK 450PF, the lower limit of its stable sintering region was chosen well above the melting region.

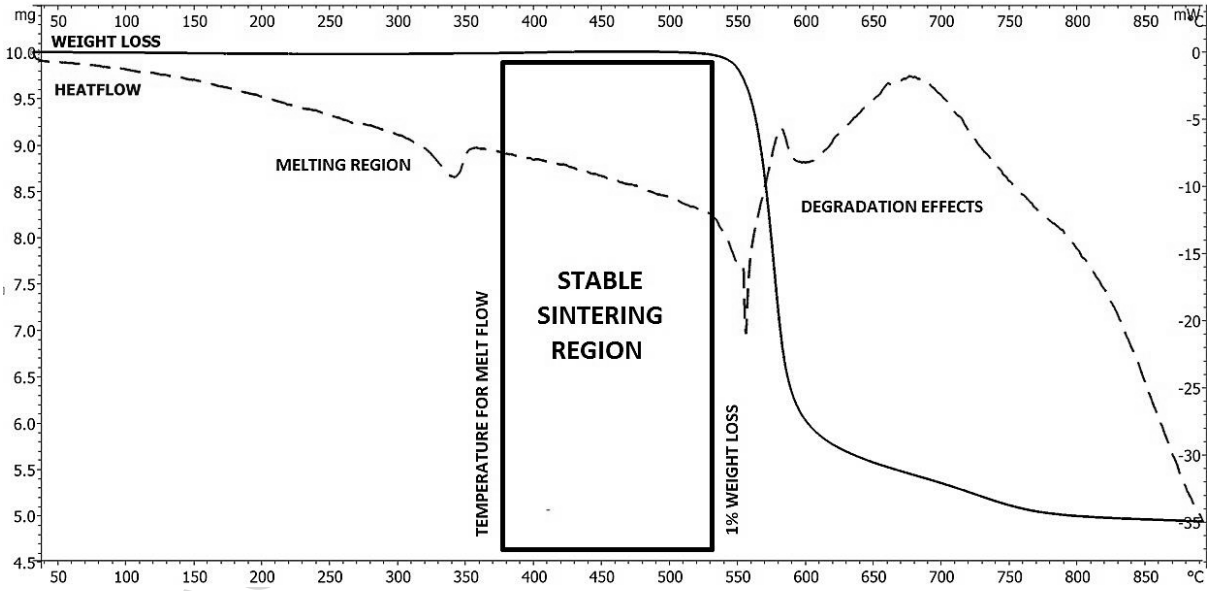

Figure 13. Stable sintering region for thermally conditioned PEEK 450PF found by combining DSC (heat flow) and TGA (weight loss) experimental data

Thermally conditioned PEEK 450PF shows a stable sintering region starting at 380˚C and finishing at 530˚C with a temperature width of 250˚C. This wide range of possible stable sintering temperatures is due to the high onset material degradation temperature, a known characteristic of the PEEK materials. Therefore the optimal processing parameters of the laser exposure strategy - laser power, scan spacing, scan count and laser speed - should be chosen to raise the temperature of the PEEK particles higher than 380 ˚C but lower than 530 ˚C. Interestingly, the stable sintering region approach seems to outline that a HT-LS material such as PEEK 450PF might offer a wider operating window in terms of laser exposure parameters than a well-established previously optimised LS material such as PA 12.

4.5 Energy Melting Ratio (EMR)

4.5.1 Activation energy

The evaluation of EMR_D was carried out for the measurement of the activation energy occurring in thermal degradation. The value of this parameter for the thermally conditioned PEEK 450PF material was calculated using the Kissinger method with several TGA experiments carried out at different heating rates (β). The results of the TGA experiments at different heating rates are shown in Figure 14, while the numerical values are listed in Table 6 along with the onset degradation temperatures at which 1% weight loss occurred.

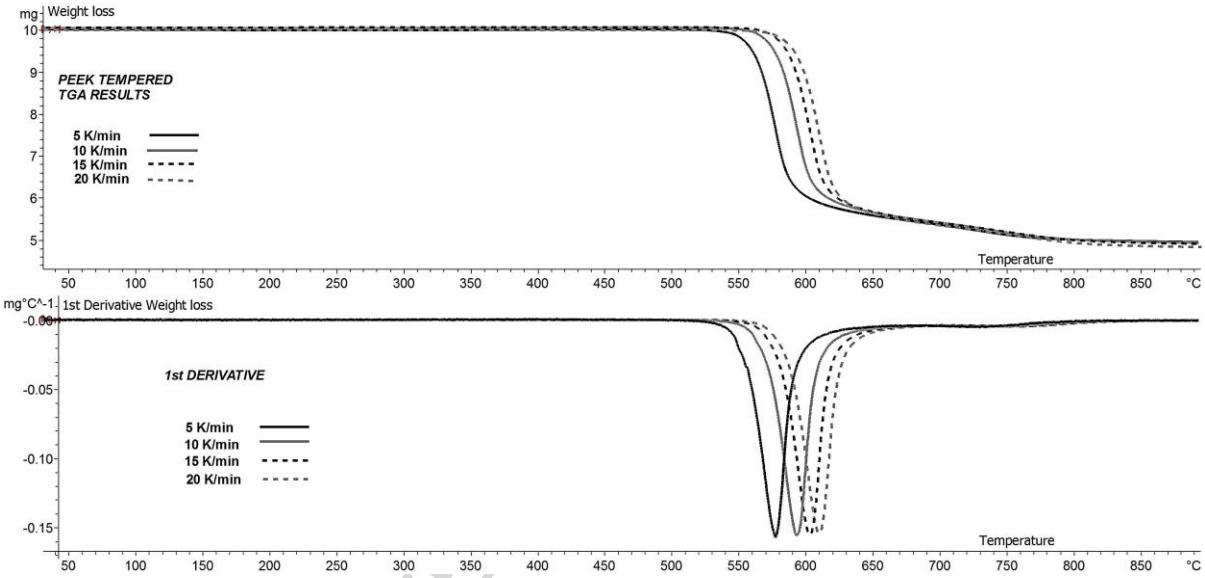

Figure 14. TGA data of thermally conditioned PEEK 450PF used for the evaluation of the activation energy

β (K min^{-1})	T_{max} (K)	T_D (K)
5	850.06	817.53
10	865.89	833.12
15	875.76	841.89
20	882.8	848.82

Table 6. TGA data used for evaluation of the activation energy with the Kissinger method for the thermally conditioned PEEK 450PF material

PEEK 450PF showed a higher degradation limit when tested at higher heating rates. Similarly, the maximum temperature of the first derivative of the TGA results (T_{max}) increases with higher heating rates. The heating rate changes the time scale of the degradation process. The lower the heating rate, the longer a material sample is kept at a range of temperature that are critical for triggering degradation, and the sooner it will then degrade. This behaviour is not surprising as it was also noticed in other polymeric specimens [41]. Figure 15 represents the Kissinger plot for PEEK 450PF grade.

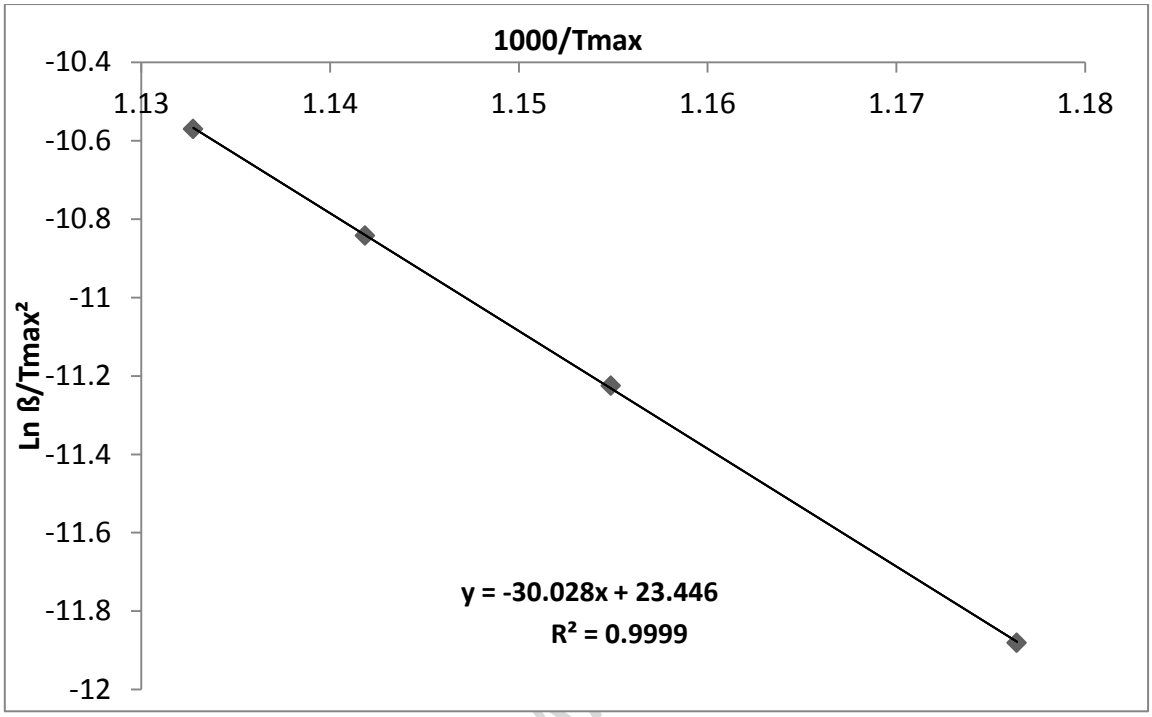

Figure 15. Kissinger plot for PEEK 450PF thermally conditioned

The activation energy of thermally conditioned PEEK 450PF has been evaluated by multiplying the coefficient of the straight line fit found in the Kissinger plot by the gas constant and has been found equal to 249.7 kJ x mol^{-1}. This value has then been used in the calculation of the EMR_D parameter.

4.5.2 Bulk density and packing fraction

The results of the bulk density (Q) and packing fraction (Φ) of thermally conditioned PEEK 450PF are reported in Table 7.

Mass of material contained in 100 cm^3 volume (g)	Bulk density (g/cm^3)	Packing fraction
78	0.385	0.292
78	0.385	0.292
77.5	0.380	0.288

Table 7. Bulk density and packing fraction data for PEEK 450PF

The average bulk density was found to be 0.383 ± 0.003 g x cm^{-3} while the packing fraction was found equal to 0.290 ± 0.002.

4.5.3 EMR value leading to thermal degradation, EMR_D

The value of the EMR leading to thermal degradation (EMR_D) and the corresponding laser power (P_D) that should cause degradation on PEEK 450PF were respectively found to be equal to 22.7 and 11.4W. The values were calculated using the parameters listed in Table 2 according to Eq. 5 and 7 respectively.

4.5.4 EMR analysis for PEEK 450PF

A plot of the tensile strength of thermally conditioned PEEK 450PF HT-LS specimens against the EMR values is shown in Figure 16. The values were calculated using the parameters listed in Table 3 according to Eq. 4. EMR_D was calculated in paragraph 4.5.3.

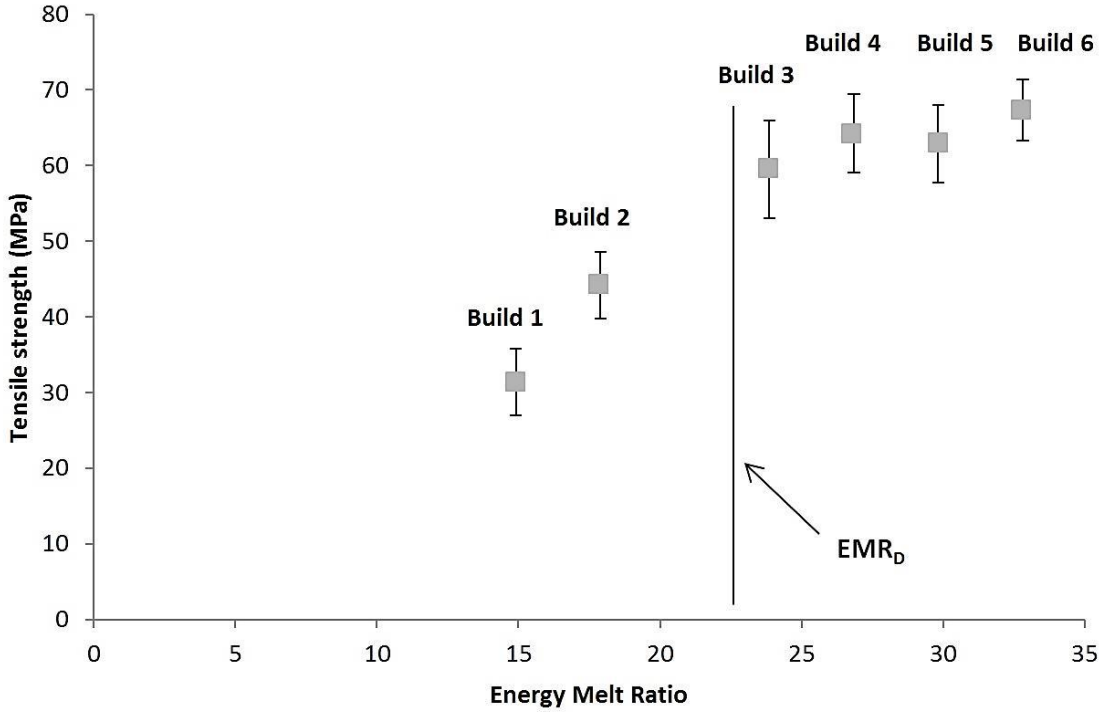

Figure 16. Tensile strength versus EMR for HT-LS specimens of thermally conditioned PEEK 450PF. EMR_D has been found to equal 22.7 with the corresponding laser power degradation approximately 11 W.

Figure 16 shows that an increase in the EMR value corresponds to increasing tensile strength values in the HT laser sintered PEEK components, until they stabilise. Clearly, the results obtained with the EMR analysis on PEEK (Figure 16) are slightly different from the trend found by Vasquez et al. [9] on the mechanical performance the PA 12 laser sintered components. PA 12 structures showed increasing values of tensile with increasing values of EMR up to a peak when they start to drop, indicating the occurrence of material degradation. The EMR_D factor was found to be a relatively good prediction of the occurrence of the drop of the mechanical properties of the PA 12 laser sintered components and therefore of the degradation during laser exposure on the basis of the powder material properties.

It is important to outline that the EMR analysis has been applied to thermally conditioned PEEK 450PF only, because virgin PEEK 450PF specimens have not been HT laser sintered and therefore not tested in terms of tensile strength. The poor spreading performance exhibited by the unconditioned PEEK 450 PF polymer in the EOSINT P 800 fully hindered further HT-LS processing of the 'as received' powder and the manufacture of tensile test samples. The EMR values of thermally conditioned PEEK 450PF (Figure 16) are much higher than the results found for PA by Vasquez et al. [9]. This difference could suggest a poor absorption of the laser energy in PEEK or could be due to the intrinsic properties of the PEEK material such as higher onset degradation temperature, lower specific heat capacity, lower enthalpy of melt and lower packing fraction than the PA 12 powder.

To further check upon the robustness of the EMR analysis, a hypothetical EMR value has been selected (EMR = 1). The laser power corresponding to EMR equal to 1 should be 0.5 W (Eq. 4). Previous results found by the authors [26] have shown that when a sample is manufactured with a

laser power of 0.85 W, the specimen is so fragile that it breaks during removal from the powder cake (Figure 17).

Figure 17. PEEK 450PF laser sintered sample manufactured with build parameters corresponding to EMR =1.

The value EMR_D of thermally conditioned PEEK 450PF has been found to equal 22.7 with corresponding P_D of approximately 11 W. This result was surprising because it implies that the PEEK material should exhibit signs of thermal degradation for processing parameters of the Build 3 (Table 1), although the specimens produced as just about reaching the plateau of maximum mechanical performance. In other words, PEEK 450PF seems to start to degrade during the HT-LS process before achieving the maximum mechanical performance. In order to understand better the EMR_D value and its real effect on HT laser sintered structures, a standard TGA has been performed on: virgin PEEK 450PF powder, thermally conditioned PEEK 450PF powder and a laser sintered sample fabricated according to the settings of Build 3 and EMR_D of 22.7. The TGA results of all the samples are shown in Figure 18.

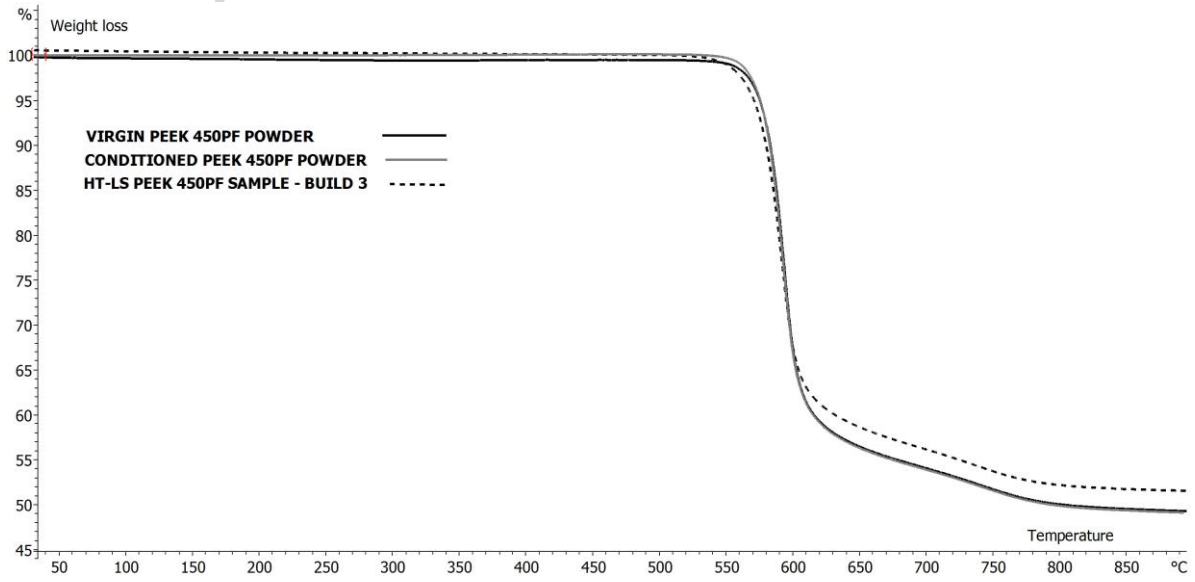

Figure 18. TGA curves of PEEK 450PF virgin and thermally conditioned powder and HT laser sintered specimen manufactured according to Build 3

The 1% weight loss degradation has been measured for all the samples, virgin and thermally conditioned powders, laser sintered specimen and are listed in Table 8. T_D is defined as the temperature at which 1% weight loss occurs because of degradation of the materials under test.

Material	T_D (˚C)
HT-LS sample – Build 3	545.78
Virgin PEEK 450PF	559.32
Thermally conditioned PEEK 450PF	561.16

Table 8. Degradation temperature causing 1% weight loss evaluated with TGA analysis performed on virgin and thermally conditioned PEEK 450PF powder and on a HT laser sintered sample manufactured with Build 3 processing parameters

The 1% weight loss degradation occurred at the same temperature for virgin and thermally conditioned PEEK 450PF powder (560 °C), indicating that no signs of thermal degradation occurred during the thermal conditioning of the powder. The HT laser sintered specimen instead showed the 1% weight loss degradation at 546 ˚C, nearly 15 ˚C lower than the powder samples. This result indicates that HT-LS process significantly affects the thermal history of the PEEK material leading to earlier degradation than in the powdered samples. However, signs of decomposition products on PEEK have been reported to appear at 450 °C [42], while colour changes were noticed after exposure for prolonged time at 400 °C [43]. It is therefore not clear whether the EMR_D shown in Figure 16 provides a good prediction of the beginning of thermal degradation phenomena in HT-LS, which occurs before the material reaches the highest tensile strength performance available through this manufacturing technique. It is possible that the 1% degradation limit (1% weight loss) could be a too strict threshold required on HT laser sintered components and, as shown in Figure 16, too little to cause a significant impact on the mechanical performance. At present a tolerance degradation value acceptable in HT-LS components has not yet been established and therefore it is not clear what degradation level can be allowed in HT-LS applications. The 1% weight loss degradation could in reality be unrequired for the success of a given HT laser sintered PEEK component unless the brittleness is increased, which could be a problem.

5 Conclusions

The general approach in the LS community for testing new polymeric powder candidates is based on performing a series of trial-and-error builds. This strategy is effective at times but very often time-consuming and expensive. A more systematic and less wasteful method would help and speed up the processability investigation of new materials and would also provide new insights into LS. In this context, a new basic technique for the prediction of the part bed processing temperature for PAEK polymers is suggested. Few previous studies attempted to develop techniques (such as the stable sintering region and the Energy Melt Ratio analysis) that can predict processing parameters and part performance based on the powder material properties. In this research work, the stable sintering region and the EMR analyses have been applied to the PEEK 450PF material. The stable sintering region technique showed a wide temperature range (250 ˚C) applicable for laser sintering of PEEK without signs of degradation. The EMR value based on 1% weight loss as equivalent to sample degradation seems not to accurately fit the results of tensile strength test of PEEK specimens. Possibly, the 1% weight loss threshold does not affect significantly the mechanical performance of the HT laser sintered samples. It is therefore clear that the EMR parameter represents a good starting point for the prediction of optimal processing parameters in HT-LS although it anticipates degradation before actual effects can be seen in the mechanical performance of the sintered parts.

A correction of the degradation limit in the calculation of the EMR_D could indeed lead to even better predictions of the optimal HT-LS processing conditions from the material properties.

6 Acknowledgements

The authors wish to acknowledge Victrex [23] and Invibio Biomaterials Solutions [44] for the supply of materials.

7 References

1. EOS, *EOSINT P 800 manual*.
2. Hopkinson, N., R.J.M. Hague, and P.M. Dickens, *Rapid Manufacturing: An Industrial Revolution for the Digital Age* 2006: John Wiley.
3. Ho, H.C.H., I. Gibson, and W.L. Cheung, *Effects of energy density on morphology and properties of selective laser sintered polycarbonate.* Journal of Materials Processing Technology, 1999. **89–90**(0): p. 204-210.
4. Drummer, D., M. Drexler, and F. Kühnlein, *Effects on the Density Distribution of SLS-Parts.* Physics Procedia, 2012. **39**(0): p. 500-508.
5. Drummer, D., D. Rietzel, and F. Kühnlein, *Development of a characterization approach for the sintering behavior of new thermoplastics for selective laser sintering.* Physics Procedia, 2010. **5, Part B**: p. 533-542.
6. Caulfield, B., P.E. McHugh, and S. Lohfeld, *Dependence of mechanical properties of polyamide components on build parameters in the SLS process.* Journal of Materials Processing Technology, 2007. **182**(1–3): p. 477-488.
7. Franco, A., M. Lanzetta, and L. Romoli, *Experimental analysis of selective laser sintering of polyamide powders: An energy perspective.* Journal of Cleaner Production, 2010. **18**(16-17): p. 1722-1730.
8. Franco, A. and L. Romoli, *Characterization of laser energy consumption in sintering of polymer based powders.* Journal of Materials Processing Technology, 2012. **212**(4): p. 917-926.
9. Vasquez, M., B. Haworth, and N. Hopkinson, *Methods for quantifying the stable sintering region in laser sintered polyamide-12.* Polymer Engineering & Science, 2013. **53**(6): p. 1230-1240.
10. Berretta, S., K.E. Evans, and O. Ghita, *Processability of PEEK, a new polymer for High Temperature Laser Sintering (HT-LS).* European Polymer Journal, 2015. **68**: p. 243-266.
11. Schmidt, M., D. Pohle, and T. Rechtenwald, *Selective Laser Sintering of PEEK.* CIRP Annals - Manufacturing Technology, 2007. **56**(1): p. 205-208.
12. Tan, K.H., et al., *Scaffold development using selective laser sintering of polyetheretherketone–hydroxyapatite biocomposite blends.* Biomaterials, 2003. **24**(18): p. 3115-3123.
13. Wendel, B., et al., *Additive Processing of Polymers.* Macromolecular Materials and Engineering, 2008. **293**(10): p. 799-809.
14. Goodridge, R.D., C.J. Tuck, and R.J.M. Hague, *Laser sintering of polyamides and other polymers.* Progress in Materials Science, 2012. **57**(2): p. 229-267.
15. Kruth, J.P., et al., *Consolidation phenomena in laser and powder-bed based layered manufacturing.* CIRP Annals - Manufacturing Technology, 2007. **56**(2): p. 730-759.
16. Kruth, J.P., et al., *Lasers and materials in selective laser sintering.* Assembly Automation, 2003. **23**(4): p. 357-371.
17. Kruth, J.-P., et al., *Binding Mechanisms in Selective Laser Sintering and Selective Laser Melting.* Rapid prototyping journal, 2005. **11**(1): p. 26-36.
18. Vasquez, M., *Analysis and development of new materials for polymer laser sintering*, 2012, Loughborough University.
19. Starr, T.L., T.J. Gornet, and J.S. Usher, *The effect of process conditions on mechanical properties of laser ‐sintered nylon.* Rapid prototyping journal, 2011. **17**(6): p. 418-423.
20. Pramoda, K.P., et al., *Characterization and thermal degradation of polyimide and polyamide liquid crystalline polymers.* Polymer Degradation and Stability, 2000. **67**(2): p. 365-374.
21. Margolis, J.M., *Engineering Thermoplastics: Properties and Applications*1985: Dekker.
22. EOS. *http://www.eos.info/en/home.html*. [cited 2015 April].
23. Victrex. *http://www.victrex.com*. [cited 2015 April].
24. Victrex, *PEEK 450 PF datasheet.*
25. Leuterer M., M.F., Pfister A., *PAEK powder, in particular for the use in a method for a layer-wise manufacturing of a three-dimensional object, as well as method for producing it*, 2012.
26. Berretta, S., *Poly Ether Ether Ketone (PEEK) polymers for High Temperature Laser Sintering (HT-LS)*, 2015, University of Exeter.
27. EOS. *PA 2200 material datasheet*.
28. EOS, *EOSINT P 100 manual.*
29. MettlerToledo, *STARe software manual*.
30. Bailey, M.L., R. Raman, and R.M. German, *Method of making a biocompatible filter*, 1997, Google Patents.
31. Victrex, *PEEK 450 G Datasheet.*
32. Schmid, M., et al. *Flowability of powders for Selective Laser Sintering (SLS) investigated by Round Robin Test*. in *High Value Manufacturing: Advanced Research in Virtual and Rapid Prototyping - Proceedings of the 6th International Conference on Advanced Research and Rapid Prototyping, VR@P 2013*. 2014.
33. Kurtz, S.M. and J.N. Devine, *PEEK biomaterials in trauma, orthopedic, and spinal implants.* Biomaterials, 2007. **28**(32): p. 4845-4869.
34. Bouzidi, L., et al., *Use of first and second derivatives to accurately determine key parameters of DSC thermographs in lipid crystallization studies.* Thermochimica Acta, 2005. **439**(1–2): p. 94-102.

35. Gabbott, P., *Principles and Applications of Thermal Analysis*2008: Wiley.
36. Bassett, D.C., R.H. Olley, and I.A.M. Al Raheil, *On crystallization phenomena in PEEK.* Polymer, 1988. **29**(10): p. 1745-1754.
37. Hsiao, B.S., et al., *Time-resolved X-ray study of poly(aryl ether ether ketone) crystallization and melting behaviour: 1. Crystallization.* Polymer, 1993. **34**(19): p. 3986-3995.
38. Hsiao, B.S., et al., *Time-resolved X-ray study of poly(aryl ether ether ketone) crystallization and melting behaviour: 2. Melting.* Polymer, 1993. **34**(19): p. 3996-4003.
39. Wang, Y., et al., *Unusual crystalline morphology of Poly Aryl Ether Ketones (PAEKs).* RSC Advances, 2016. **6**(4): p. 3198-3209.
40. Tan, K.H., et al., *Fabrication and characterization of three-dimensional poly (ether-ether-ketone) / hydroxyapatite biocomposite scaffolds using laser sintering.* Proceedings of the Institution of Mechanical Engineers, Part H: Journal of Engineering in Medicine, 2005. **219**(3): p. 183-194.
41. Sichina, W.J. *Characterization of Polymers Using TGA*. [cited 2015 May]; Available from: http://depts.washington.edu/mseuser/Equipment/RefNotes/TGA_Notes.pdf.
42. Patel, P., et al., *Mechanism of thermal decomposition of poly(ether ether ketone) (PEEK) from a review of decomposition studies.* Polymer Degradation and Stability, 2010. **95**(5): p. 709-718.
43. Day, M., D. Sally, and D.M. Wiles, *Thermal degradation of poly(aryl-ether-ether-ketone): Experimental evaluation of crosslinking reactions.* Journal of Applied Polymer Science, 1990. **40**(9-10): p. 1615-1625.
44. InvibioBiomaterialSolutions. *http://www.invibio.com/*. [cited 2015 April].

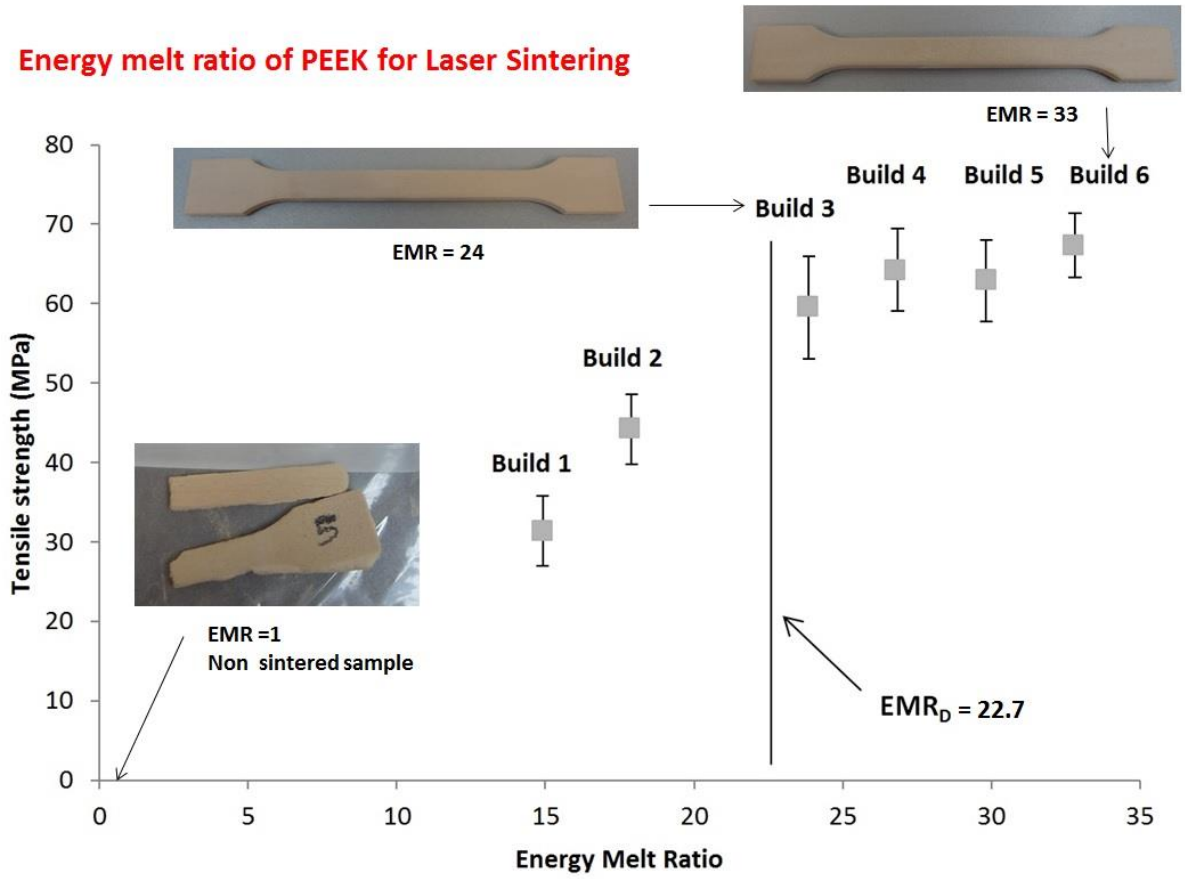

Graphical Abstract

Highlights

- This work provides new insights into the thermal behaviour of new materials for high temperature laser sintering
- The study defines the stable sintering region for laser sintering of PEEK
- The mechanical properties of laser sintered PEEK specimens are not affected by the 1% thermal degradation limit predicted by the energy melt ratio parameter
- A new technique to predict the part bed temperature of high temperature polymers from powder properties is suggested